

On the Origin of X-ray Emission From Millisecond Pulsars in 47 Tuc

K. S. Cheng¹ and Ronald E. Taam²

¹ *Department of Physics, University of Hong Kong, Pokfulam Road, Hong Kong*

² *Department of Physics & Astronomy, Northwestern University, Evanston, IL 60208*

ABSTRACT

The observed spectra and X-ray luminosities of millisecond pulsars in 47 Tuc can be interpreted in the context of theoretical models based on strong, small scale multipole fields on the neutron star surface. For multipole fields that are relatively strong as compared to the large scale dipole field, the emitted X-rays are thermal and likely result from polar cap heating associated with the return current from the polar gap. On the other hand, for weak multipole fields, the emission is nonthermal and results from synchrotron radiation of e^\pm pairs created by curvature radiation. The X-ray luminosity, L_x , is related to the spin down power, L_{sd} , expressed in the form $L_x \propto L_{sd}^\beta$ with $\beta \sim 0.5$ and ~ 1 for strong and weak multipole fields respectively. If the polar cap size is of the order of the length scale of the multipole field, s , the polar cap temperature is $\sim 3 \times 10^6 K \left(\frac{L_{sd}}{10^{34} \text{ergs}^{-1}} \right)^{1/8} \left(\frac{s}{3 \times 10^4 \text{cm}} \right)^{-1/2}$.

A comparison of the X-ray properties of millisecond pulsars in globular clusters and in the Galactic field suggests that the emergence of relatively strong small scale multipole fields from the neutron star interior may be correlated with the age and evolutionary history of the underlying neutron star.

Subject headings: pulsars: general — radiation mechanisms: thermal — radiation mechanisms: nonthermal — X-rays: stars

Accepted for publication in ApJ.

1. INTRODUCTION

The discovery of millisecond pulsars (MSPs) as a class of rapidly rotating ($P < 10$ ms), weakly magnetized ($B \lesssim 10^{10}$ G) neutron stars has stimulated considerable interest in the

fundamental properties of these objects. The detailed observational study of these sources over periods of time have provided insights into their origin and evolution in close binary systems (see for example, Phinney & Kulkarni 1994). The hypothesis that MSPs are neutron stars recycled in a spin up phase during which angular momentum and mass are accreted from a companion star (Radhakrishnan & Srinivasan 1982; Alpar et al. 1982) has been dramatically confirmed with the observational detection of the four millisecond accreting X-ray pulsars J1808.4-3658 (Wijnands & van Klis 1998), J1751-305 (Markwardt et al. 2002), J0929-314 (Galloway et al. 2002), and J1807-294 (Markwardt, Smith, & Swank 2003). Their combination of short spin period and low dipole magnetic field strengths have, furthermore, provided important clues on the temporal evolution of magnetic fields in neutron stars in low mass X-ray binary systems (van den Heuvel, van Paradijs, & Taam 1986; see also Bhattacharya 2002 for a recent review).

Insights into the nature of the emission mechanisms have been facilitated by observational investigations over broad spectral regions. As an example, the early X-ray studies of MSPs using the ROSAT satellite revealed that the MSPs in the Galactic field appear to have a non thermal character (see Becker & Trümper 1997, 1999) with a power law photon index ranging from ~ -2 to -2.4 . On the other hand, the recent X-ray studies with the Chandra satellite by Grindlay et al. (2002) indicate that the MSPs in 47 Tuc appear to be consistent with a thermal black body spectrum characterized by a temperature corresponding to an energy of 0.2 - 0.3 keV.

Additional evidence supporting the apparent difference between the MSPs in the Galactic field and in 47 Tuc and, hence difference in their fundamental properties, can be gleaned from the relation between the X-ray luminosity, L_x , and the spin down power, L_{sd} , expressed in the form $L_x \propto L_{sd}^\beta$. Using ROSAT data Becker & Trümper (1997, 1999) found that $\beta \sim 1$ for MSPs in the Galactic field, whereas there are hints that the dependence is shallower ($\beta \sim 0.5$) for the MSPs in 47 Tuc (see Grindlay et al. 2002). An existence of a correlation between these two quantities provides strong evidence for relating the energy source of the X-ray emission to the rotational energy of the underlying neutron star. We shall, for convenience, group the MSPs with properties similar to the Galactic field as Type I and those similar to the MSPs in 47 Tuc as Type II, even though the nearest MSP J0437-4715 has an X-ray spectrum consisting of two thermal components and one non thermal component (Zavlin et al. 2002).

The conversion of rotational energy to X-ray radiation in these MSPs is likely produced by electromagnetic processes in the neutron star's magnetosphere (e.g., Halpern & Ruderman 1993) rather than by frictional processes in its interior (Alpar et al. 1984; Shibazaki & Lamb 1988). In this case, the emission can take place either at the magnetic poles (Daugherty &

Harding 1996) or in the outer magnetosphere (Cheng, Ho, & Ruderman 1986). Specifically, it has been argued that the non thermal X-ray emission of rotation powered pulsars results from the synchrotron radiation of e^\pm pairs created in the magnetosphere near the neutron star surface by curvature photons. Such photons are emitted by charged particles on their way from the outer magnetospheric gap to the neutron star surface (Cheng, Gil & Zhang 1998; Cheng & Zhang 1999). The non thermal X-ray luminosity is roughly about 0.1% of the spin-down power. We note, however, that the presence of a complicated surface magnetic field can change the character of the emission since the open field lines, where the outer magnetospheric gap is located, can curve upward. In this case e^\pm production and outflow can occur on all open field lines and, hence, quench the outer magnetospheric gap (Ruderman & Cheng 1988). Observational evidence in support of emission taking place in the magnetosphere is suggested by the existence of pulsed emission in both the radio and soft X-ray region of the 5.75 ms pulsar J0437-4715 (Becker & Trümper 1999).

On the other hand, thermal X-ray radiation can be produced by either neutron star cooling (Tsuruta 1998) or polar cap heating (Arons 1981; Harding, Ozernoy & Usov 1993). Since MSPs are extremely old pulsars, the internal heating mechanisms lead to surface temperatures $\lesssim 10^5$ K (Alpar et al. 1984; Shibazaki Lamb 1989; Cheng et al. 1992). Hence, the blackbody thermal emission observed from the MSPs in 47 Tuc should be attributed to polar cap heating associated with the impact of the return current of high energy electrons, perhaps produced in the inner or outer gaps of the magnetosphere (see Cheng, Gil, & Zhang 1997; Cheng & Zhang 1999), on the neutron star surface.

However, although the X-ray emission from MSPs in the Galactic disk is dominated by non thermal emission, the pulsed fraction, in cases that can be determined, is usually less than 50%. For example, the pulsed-fraction of PSR J2124-3358 is 55% in ASCA energy range and 33% in ROSAT energy range respectively (Sakurai et al. 2001; Becker & Trümper 1999). Furthermore, Stappers et al. (2003) have reported an X-ray nebula associated with PSR 1957 +20. Therefore it is possible that a significant fraction of non thermal X-ray emission may come from an unresolved nebular component around the pulsar. According to the observed results of Stappers et al. (2003), this unresolved X-ray emission likely represents the shock where the winds of the pulsar and its companion collide. Grindlay et al. (2002) have also suggested that the MSP in NGC6397 may have such a contribution as well. On the other hand, many MSPs in 47 Tuc have a binary companion, but their X-ray emissions are still dominated by a thermal spectrum. Furthermore, Tennant et al. (2001) have detected X-ray emission from the Crab pulsar at the pulse minimum. This indicates that some unpulsed-fraction can originate from the pulsar magnetosphere. We believe that although it is possible that the nebula may contribute to the non thermal emission, perhaps resulting in a spectral difference between MSPs in the disk and in 47 Tuc, the observed

results have not yet provided compelling evidence to support this conjecture.

Since the spin period, binary period, X-ray luminosity, and estimated dipole magnetic field of the two groups of MSPs overlap, other differences in properties must be sought to explain the dichotomy. Recently, Grindlay et al. (2002) suggested that their differences may be related to either the existence of high order multipole fields on the neutron star surface or to the formation of higher mass neutron stars in the dense cluster environment of 47 Tuc. The small radius of curvature associated with high order fields can facilitate the production of e^\pm pair formation close to the neutron star surface and to an increased efficiency of polar cap heating with a corresponding increase in the level of thermal X-ray emission. Higher mass neutron stars are more compact and can prolong the effectiveness of the inverse Compton scattering of thermal photons from the neutron star surface in facilitating pair production (see Harding, Muslimov, & Zhang 2002) for MSPs with spin down ages $\gtrsim 10^8$ yr. Such a scattering process can lead to the relation $L_x \propto L_{sd}^{1/2}$, however, the emission resulting from this latter process is distinctly non thermal.

We suggest, in this paper, that a small scale, strong surface magnetic field may play a crucial role in determining the X-ray emission properties of MSPs. The existence of such a magnetic field may sensitively depend upon the formation history of MSPs possibly providing an explanation for the differences between the MSPs in the field and in globular clusters. In the next section we examine the hints provided by the observed features of MSPs. The generic features of polar cap heating models related to the characteristic properties of the X-ray spectrum and to the relation between its X-ray luminosity and spin down power are presented in §3. In §4, we compare the observed properties of MSPs and suggest that a possible factor differentiating these two types of MSPs is their age. The origin and evolution of multipole magnetic fields in neutron stars is discussed within the context of the emission models in §5. Finally, we summarize and discuss the implications of our study in the concluding section.

2. HINTS FROM OBSERVED FEATURES OF MSPS

In the past decade, there has been significant progress in detecting and understanding X-ray emission from rotation powered pulsars. The X-ray data obtained from the ROSAT, ASCA, RXTE, BeppoSAX, Chandra and XMM-Newton satellite observatories have provided very important constraints on theoretical models. For example, Becker & Trümper (1999) presented results of soft X-ray emission from 10 MSPs in a reanalysis of archival ROSAT data, concluding that the close correlation between the pulsar’s spin-down power and the observed X-ray luminosity suggested rotation as the energy source for the bulk of the observed non

thermal X-rays. The linear relation between the X-ray and spin-down luminosity among MSPs ($L_x \propto L_{sd}$) is consistent with that found in normal radio pulsars (Becker & Trümper 1997). The non thermal spectral features of some MSPs have also been reported by Saito et al. (1997) and Takahashi et al. (2001) based on ASCA observations and by Mineo et al. (2000) based on BeppoSax observations. Although the X-ray luminosity is dominated by the non thermal component, composite spectra (power law plus black body with temperature around a few million degrees) clearly give a better fit for the observed spectrum. However, the exact contribution of the thermal component to the X-ray luminosity is difficult to determine.

Recently, Grindlay et al. (2002) presented a homogeneous data set of MSPs in 47 Tuc observed with Chandra. This data provides a good estimate of the X-ray luminosities and color temperatures of MSPs in 47 Tuc because these pulsars are located at a common distance and therefore have a common interstellar column density. This is in contrast to the field where the uncertainties are greater. Although the MSPs in globular clusters share these common quantities, the gravitational acceleration of the globular cluster on the MSPs contaminates the measurement of the period derivative, \dot{P} . For example, about half of the MSPs in 47 Tuc have negative \dot{P} (Freire et al. 2001). While it is possible to obtain the intrinsic \dot{P} after subtraction of the gravitational effect of the cluster by numerical modelling (see Grindlay et al. 2002) the uncertainties in the intrinsic \dot{P} of an individual MSP can be large compared to the uncertainties in the average intrinsic value of all the MSPs in the cluster.

Here, we show that useful information can still be gleaned from the observed data based upon general considerations. In particular, the mean spin-down power of MSPs in 47 Tuc can be estimated from the typical age of these MSPs. An upper limit to their age is given by the age the cluster, which is estimated to be $\sim 11 - 13$ Gyr (Schiavon et al. 2002) based on spectroscopy and the cluster's color-magnitude diagram. A more realistic age estimate could be derived from the age of their white dwarf companions. Recently, Hansen, Kalogera & Rasio (2003) suggest that the typical age of helium white dwarfs in 47 Tuc should be < 2.7 Gyr. This age gives the mean spin-down power as $\langle L_{sd} \rangle \sim \frac{I \langle \Omega^2 \rangle}{2} / 2.7 \text{ Gyr} \sim 2 \times 10^{34}$ erg s $^{-1}$, where I is the moment of inertia taken to be equal to 10^{45} g cm 2 and $\langle \Omega \rangle$ is the average rotational angular frequency of the MSPs. The mean observed X-ray luminosity of MSPs in 47 Tuc is $\langle L_x \rangle = 1.95 \times 10^{30}$ erg s $^{-1}$ (cf. Table 1 of Grindlay et al. 2002) and the ratio of these quantities is $\sim 10^{-4}$. Becker & Trümper (1997, 1999) found that this ratio for normal radio pulsars as well as for MSPs, but not including MSPs in 47 Tuc is significantly larger ($\sim 10^{-3}$).

If L_x is assumed to correlate with L_{sd}^β , it implies that $L_x \propto B^{2\beta} P^{-4\beta}$ where B is the

dipolar magnetic field strength and P is the spin period. We note that the dependence of the X-ray luminosity is more sensitive to the spin period than to the magnetic field. In Figure 1, L_x is illustrated as a function of $1/P^2$. The circles are MSPs in 47 Tuc, the triangles are MSPs excluding those in 47 Tuc, and the squares are normal radio pulsars. By fitting these three sets of data by linear regression, the slopes are 0.49 ± 0.21 , 2.16 ± 0.82 and 1.82 ± 0.45 with correlation coefficients of 0.55(15), 0.71(9) and 0.71(18), where the value within the parentheses corresponds to the number of degrees of freedom. The correlation coefficients imply that the chances of probability are 0.0335, 0.03282, and 8.7×10^{-4} respectively. Obviously, the data is very scattered due to the variation of magnetic field and, hence, the chances of probability are not very significant. However, the slopes of normal radio pulsars and MSPs in the field are consistent with each other, whereas the slope of MSPs in 47 Tuc is clearly different.

The expected polar cap temperature of MSPs in 47 Tuc can be estimated as $T_{exp} \sim \left(\frac{\langle L_x \rangle}{\sigma_B \langle A_p \rangle} \right)^{1/4} < 10^6 K$ where $\langle A_p \rangle = \pi \frac{R^3 \langle \Omega \rangle}{c}$ is the mean polar cap area inferred for a dipolar magnetic field. Here, R is the radius of the neutron star. The inferred color temperature is $\sim 3 \times 10^6$ K, implying that the polar cap area is about a hundred times less than the expected value. The presence of a much smaller scale magnetic field on the neutron star surface could be consistent with this result.

Finally, we re-emphasize that L_x is dominated by the non thermal component for normal radio pulsars as well as for MSPs in the field whereas L_x is dominated by a black body thermal component for MSPs in 47 Tuc. Taken as an aggregate, these four distinguishing features suggest that the MSPs in 47 Tuc are very distinct from their Galactic field counterparts.

In next section, we review several model predictions for the X-ray luminosities, which must depend on the pulsar parameters, i.e. spin period and dipolar magnetic field strength. Although the fields of the MSPs in 47 Tuc are somewhat uncertain due to the gravitational effect of the cluster, one can roughly estimate their values. For example, Grindlay et al. (2002) have used the King model to subtract the gravitational effect of the cluster to obtain an estimate of the dipolar field of each MSP in 47 Tuc. The errors in \dot{P} are estimated to be +0.3/-0.1 in the log, which provides the error estimates in the magnetic fields used for the calculation of the X-ray luminosities shown in Table 1 (see §3). Friere et al. (2001) has adopted a more conservative approach and has provided upper limits of B for each MSP. In Figure 2, the observed L_x versus BP^{-2} is illustrated. The circles use the field estimates of Grindlay et al (2002) and the dots use the upper limit of Friere et al. (2001). The slopes of these two set of data are 0.92 ± 0.20 , and 0.89 ± 0.18 with correlation coefficients of 0.78(15) and 0.81(15), which imply that the chances of probability are 5.8×10^{-4} and 2.8×10^{-4} respectively. Considering Figure 1 and Figure 2 together, it appears that L_x is

likely proportional to P^{-1} to P^{-2} but the latter is more favorable because the probability of such a chance occurrence from an ensemble of systems is low.

3. GENERIC FEATURES OF POLAR CAP HEATING MODELS

There is a clear indication from the observed data that the spectrum of MSPs in 47 Tuc is thermal. However, thermal emission resulting from residual heat or frictional processes in the interior of old neutron stars is insufficient. The primary mechanism for MSPs, therefore, very likely involves polar cap heating. In this section, we review the various polar cap heating models and compare their general features with the observed data. Among the great number of models that have been developed to explain the pulsar radio emission, a large fraction involve an acceleration region located near the polar cap known as the polar gap or inner gap. Charged particles are accelerated to relativistic energies in the polar gap, whose potential drop is limited by pair creation. Coherent radio emission could result from the two stream instability of the faster primary charged particle beam and the slower secondary pair beam (for a general review, see Michel 1991). Some of these pairs created inside the polar gap can be separated by the electric field, resulting in a backflow current. In general, the polar cap heating can result from this backflow current, J_b , striking the polar caps. The X-ray luminosity is, therefore, simply given by

$$L_x = J_b V_{gap} \quad (1)$$

where V_{gap} is the potential difference of the polar gap. Although the exact backflow current to each polar cap is not known, it should be of the order of the Goldreich-Julian current (Goldreich & Julian 1969), which can be written as

$$J_{GJ} = 1.35 \times 10^{30} B_{12} P^{-2} e s^{-1} \quad (2)$$

where e is the charge of electron and B_{12} is the magnetic field in units of 10^{12} G. In other words,

$$J_b = \alpha J_{GJ} \quad (3)$$

where α is a model dependent parameter. For a uniform pair production situation inside the polar gap, $\alpha \sim \frac{1}{2}$. However, this factor could be further reduced if the current is concentrated in sparks rather than uniformly over the polar cap (Cheng & Ruderman 1980; Gil & Sendyk 2000) or the electric field in the pair creation region is actually weaker than in other regions (Arons 1981), which is supported by statistical analysis (e.g. Fan, Cheng & Manchester 2001).

The predicted luminosity of the thermal X-ray radiation is rather model-dependent since there exist a wide range of models for the polar gap potential difference. Here, we discuss two classes of polar gap models which depend upon whether the polar gap is sensitive or insensitive to the pulsar parameters (viz., spin period and dipolar magnetic field). Models representative of the first group are those described by Arons (1981) and Harding & Muslimov (2001). Specifically, Arons (1981) assumed the free emission of electrons (outflow) from the stellar surface with the polar cap heating resulting from the trapped positrons (inflow) in the acceleration zone (the polar gap) bombarding the stellar surface. The X-ray luminosity caused by this bombardment is estimated as

$$L_x^A \sim 2 \times 10^{26} B_{12} P^{-27/8} f_p^{-1/4} \text{erg s}^{-1} \quad (4)$$

where $f_p = 921 P^{1/2} s_5^{-1}$ is the ratio of the dipole radius of curvature to the actual radius of curvature s_5 (in units of 10^5 cm). Harding & Muslimov (2001) have included the frame dragging effect in the emission of electron polar gap models (Scharlemann, Arons & Fawley 1978; Arons & Scharlemann 1979) and predict the thermal X-ray luminosity from the polar cap as

$$L_x^{HM}(R) = 10^{-5} L_{sd} P^{-1/2} \tau_6^{3/2} \quad (5)$$

if resonant inverse Compton scattering mechanism is dominant otherwise

$$L_x^{HM}(NR) = 10^{-5} L_{sd} P^{1/2} \tau_6 \quad (6)$$

where the spin down power of the pulsar is given by

$$L_{sd} = 3.8 \times 10^{31} B_{12}^2 P^{-4} \text{erg s}^{-1}, \quad (7)$$

and τ_6 is the characteristic age of the pulsar $\frac{P}{2\dot{P}}$ in units of 10^6 yr.

Another class of models predicts thermal X-ray luminosities similar to each other because the polar gap potentials in these models are insensitive to the pulsar parameters. For example, in the situation where ions are bound to the polar cap surface (Ruderman & Sutherland 1975)

$$V_{RS} = 10^{12} B_{12}^{-1/7} P^{-1/7} s_6^{4/7} \text{volts.} \quad (8)$$

where s_6 is the radius of curvature of the surface magnetic field in units of 10^6 cm. In the presence of a strong surface magnetic field, Gil and his co-workers (Gil & Mitra 2001; Gil & Melikidze 2002) show that the Ruderman-Sutherland potential should be modified as

$$V'_{RS} = \zeta^{1/7} b^{-1/7} V_{RS} \text{volts.} \quad (9)$$

where ζ is the general relativistic correction factor, which is about 0.85 for typical neutron star parameters; $b = B_s/B_d$, where B_s is the surface magnetic field and B_d is the inferred dipolar field from the observed spin period and period derivative.

In the superstrong magnetic field $B > 0.1B_q \approx 5 \times 10^{12}\text{G}$, the high energy photons with energy E_γ will produce electron and positron pairs at or near the kinetic threshold (Daugherty & Harding 1983). Here $E_\gamma = 2mc^2/\sin\theta$ and $\sin\theta = l_{ph}/s$ where l_{ph} is the photon mean free path for pair formation. Cheng and Zhang (1999) argued that if the surface magnetic field is sufficiently localized then $\sin\theta = l_{ph}/s \sim 1$ and the minimum condition for the magnetic pair production is simply $E_\gamma > 2mc^2$ instead of $\frac{E_\gamma B}{2mc^2 B_q} > \frac{1}{15}$ (Ruderman & Sutherland 1975). This assumption yields

$$V_{CZ} = 1.6 \times 10^{11} s_6^{1/3} \text{volts.} \quad (10)$$

The Goldreich-Julian current will be dominated by the ion flow when the polar cap temperature T is higher than the critical temperature

$$T_i = 10^5 \eta B_{12}^\delta K, \quad (11)$$

where the coefficients η and δ are model dependent parameters. Jones (1986) obtained $\eta = 0.7$ and $\delta = 0.7$ respectively, whereas Abrahams & Shapiro (1991) and Usov & Melrose (1995) gave $\eta = 3.5$ and $\delta = 0.73$ respectively. In this case, the potential of a warm polar cap was suggested to be determined by the space charge limited flow of ions due to the finite inertia of ions (Cheng & Ruderman 1977; Arons & Scharlemann 1979). However, ions stream out from a warm neutron star surface ($kT < 10\text{KeV}$), and the photoejection of the most tightly bound electrons of ions (Jones 1980) acts like the electron and positron creation mechanism to reduce the potential of the polar gap to

$$V_J = \gamma(A/Z)10^9 \text{volts,} \quad (12)$$

where γ is the Lorentz factor of ions and A/Z is the ratio of atomic weight and atomic number. Typically $\gamma \sim 10$ is required to photoeject the innermost electrons. It should be noted that all these potentials (eqs.8, 9, 10 and 12) are insensitive to the pulsar parameters. If the return current is proportional to the Goldreich-Julian current, the functional dependence of the model luminosities on pulsar parameters predicted by these potentials is close to $B_{12}P^{-2}$.

Cheng & Ruderman (1980) argued that although the return current is difficult to determine, the ion flow depends on the surface temperature exponentially. It is possible that the return current and ion flow can adjust the surface temperature so that it is always near the critical temperature T_i shown in equation (11). They estimated the X-ray luminosity as $L_x = \sigma_B T_i^4 A_p$ where A_p is the polar cap area. If A_p is the dipolar area, the model X-ray luminosity is

$$L_x^{CR} = 3.7 \times 10^{24} \eta^4 B_{12}^{4\delta} P^{-1} \text{erg s}^{-1}. \quad (13)$$

In Table 1, we compare the model predicted X-ray luminosities and the observed data. Unless the estimates of dipolar magnetic fields are totally incorrect, models L_X^{RS} , L_X^{CR} ,

$L_X^{HM}(R)$ and $L_X^{HM}(NR)$ are inconsistent with the observed data. The model X-ray luminosities are higher (lower) than the observed values by more than an order of magnitude. We have adopted $s \sim 500$ m, which is the typical dimension of the stellar crust for realistic equations of state (Cheng & Dai 1997) rather than the dipolar radius of curvature. This choice is motivated by the work of Arons (1993), who suggested that the surface magnetic field should be a superposition of clumps covering the entire surface of the neutron star. Further support for such a choice is suggested by the study of Ruderman (1991a,b), who argued that the surface magnetic field of pulsars should have a sunspot-like clump structure. Because the core of the neutron star is liquid, it is natural that the size of these clumps should be about the thickness of the solid crust. In the model developed by Jones (1980), the radius of curvature does not enter explicitly in the potential, but implicitly through the Lorentz factor. In this case

$$\gamma \approx \frac{10KeV}{3kT_{cap}(1 - \cos\theta_x)}, \quad (14)$$

where T_{cap} is the polar cap temperature, which is $\sim 2.6 \times 10^6$ K (Grindlay et al. 2002) and $\theta_x \sim \frac{h}{s}$ is the angle between the X-ray photon and the local magnetic field with h corresponding to the height of the polar gap. If the radius of curvature is the dipolar value, then $\gamma \sim 10^3$, and this will not be an important mechanism to limit the potential of the polar gap. However, assuming that s is small and hence $(1 - \cos\theta_x) \sim 1$, the potential is limited by the polar cap temperature. In this approximation, we choose $\gamma \approx \frac{10KeV}{3kT} \approx 20$ and $A/Z \approx 2$. for the model calculations.

Actually L_x^{CR} and $L_x^{HM}(R)$ can be consistent with the observed values for a much stronger dipolar surface magnetic field ($B_{12} > 1$). However, the predicted surface temperature T_i of model L_x^{CR} is still significantly lower than the observed value by an order of magnitude. L_x^{RS} can be also consistent with the observed values if the return current is significantly lower than the Goldreich-Julian current.

In fact, all models with the predicted L_x^{model} consistent with L_X^{obs} require the existence of a strong multipole field on the stellar surface including L_x^A . In calculating L_x^A , we have assumed the actual radius of curvature $s \sim 500m$. If s is dipolar, L_x^A will increase by a factor of ~ 10 , which makes the model predicted luminosity higher than the observed luminosity by an order of magnitude.

With the exception of L_x^A , all model X-ray luminosities discussed here depend on $1/P^\delta$ with δ between 1 and 2, which approximately reproduces the observed data. However, if the magnetic field dependence is included only models L_x^{RS} , L_x^{CZ} and L_x^J give the correct dependence on $\sim B/P^2$. These three models require small scale, strong surface magnetic fields $> 10^{12}$ G, at least near the polar cap but not necessarily over the entire stellar surface. This strong surface magnetic field also implies that the polar cap area is determined by

the length dimension of the surface field instead of the dipolar area. For a length scale of the multipole field s , the polar cap temperature is $\sim 3 \times 10^6 K \left(\frac{L_{sd}}{10^{34} \text{ergs}^{-1}} \right)^{1/8} \left(\frac{s}{3 \times 10^4 \text{cm}} \right)^{-1/2}$, which is relatively insensitive to the spin down power and consistent with the observed data.

4. OBSERVATIONAL PROPERTIES OF MSPS

As described previously, the Type I and Type II MSPs are distinct in their X-ray characteristics, but their overall timing properties are common. For example, the spin periods of the Type I X-ray sampled MSPs range from 1.56 ms - 5.26 ms (Grindlay et al. 2002) and those of the Type II X-ray sampled MSPs range from 2.1 ms - 7.59 ms (Camilo et al. 2000). The orbital periods of those MSPs in binary systems also span a common range as well lying between 0.38 d - 5.74 d for Type I (see Taam, King, & Ritter 2000) and 0.12 d - 2.36 d for Type II (Camilo et al. 2000). Although the determination of the spin period derivative of Type II MSPs is contaminated by accelerations in the globular cluster gravitational potential, the upper limits for the surface dipole magnetic fields of $\lesssim 10^9$ G (Freire et al. 2001) are similar in magnitude to Type I MSPs (with B in the range from $10^8 - 10^9$ G). Thus, upon comparison of these observed and inferred properties there are no apparently distinguishing characteristics to differentiate the X-ray properties of these two groups.

The masses of the neutron star could be different between the two groups, but the metallicity of 47 Tuc (with $[\text{Fe}/\text{H}] = -0.7$) does not significantly differ from that of the Galactic disk to affect the properties of the neutron star (see Woosley, Heger, & Weaver 2002). On the other hand, tidal capture (Bailyn & Grindlay 1987) and exchange collisions (Rasio, Pfahl, & Rappaport 2000) followed by a common envelope phase can provide additional channels for the formation of binary MSPs in globular clusters. However, the various evolutionary scenarios for the formation of MSPs in the Galactic field (Taam et al. 2000) do not necessarily lead to systematically different neutron star masses in the Type I group in every single case. In fact, the fundamental issue of whether the neutron star's mass is significantly increased during the LMXB phase is inconclusive since the amount of matter accreted can depend on whether mass loss from the system is significant during a phase when the accretion disk surrounding the neutron star is thermally unstable (cf., Li 2002; Podsiadlowski, Rappaport, & Pfahl 2002).

Given that there are no clear distinguishing characteristics between the neutron stars in the MSPs in the Type I and Type II groups, we consider the hypothesis that age is a possible discriminating factor. Neutron stars in globular clusters are likely to be older than their counterparts in the Galactic field. MSP formation in globular clusters is likely to differ from that in the Galactic field since the long period primordial binaries (which

are the prime progenitors of short binary period MSPs in the Galactic field) are soft in the cluster environment and, hence, can be disrupted by stellar encounters (Heggie 1975; Hut 1984; Taam & Lin 1992). Therefore, the neutron stars that are present as MSPs in a globular cluster are likely to have been isolated for as long as several Gyr, after which they underwent an exchange collision or tidal capture to form a close interacting binary system. The subsequent spin up evolution during an accretion phase and the spin down evolution during the post accretion phase is not likely to be dissimilar to those neutron stars in MSPs in the Galactic field. Since the MSPs in the Type I group form from primordial binaries, in contrast to those in Type II, the neutron stars in short orbital period systems that are the primary focus of this study are likely to have a relatively short pre accretion phase determined by the main sequence turnoff timescale of its binary companion. If we assume that the short period binary MSPs are formed via the common envelope phase (for a review, see Taam & Sandquist 2000) directly from a progenitor system containing an intermediate mass companion (Podsiadlowski et al. 2002), then an upper limit on the duration of the pre accretion phase for MSPs of Type I can be estimated, for example, to be $\lesssim 10^8$ yr for $\sim 3 M_{\odot}$ companion.

The age of the neutron star as a MSP, however, corresponds to the time since the accretion phase ceased and can be estimated from the characteristic pulsar age given by the spin down timescale, $\frac{P}{2\dot{P}}$ for a braking index equal to 3. We note that this age is only an upper limit since the spin period at the cessation of the accretion phase may not significantly differ from its present day spin period. For the MSPs in 47 Tuc, the uncertainties of their characteristic ages are large and not as reliable as those inferred for the MSPs in the Galactic field.

An observational clue for differentiating the MSPs in the two groups is provided by the existence of 3.05 ms MSP B1821-34 in the globular cluster M28 (Lyne et al. 1987). In contrast to the MSPs in 47 Tuc, the X-ray emission from B1821-34 is distinctly non thermal (Becker & Trümper 1997) and $L_x \propto L_{sd}$. However, its short spin down age amounting to less than 3×10^7 years distinguishes it from the other MSPs in the Type II group. Since its spin down timescale is much less than any of the spin down timescales estimated for the MSPs in 47 Tuc (see Grindlay et al. 2002), it is highly suggestive that the neutron star age as a MSP is one factor which may help to distinguish MSPs in Type I from those in Type II.

The 3.65 ms pulsar PSR J1740-5340 in the globular cluster NGC 6397 (D’Amico et al. 2001) can also provide a similar constraint, however, it is unclear whether it belongs to either of these two groups since its X-ray spectrum is non thermal, but yet it appears that $L_x \propto L_{sd}^{1/2}$. This source is unique in that it is an eclipsing MSP and the observations of

nonvanishing emission during eclipse (Grindlay et al. 2002) suggest that the emission region is extended. As a result, the X-ray emission may not solely reflect processes taking place in the immediate vicinity of the neutron star surface and the inferences drawn from J1740-5340 are inconclusive.

The pulse timing properties MSPs in the Type I group reveal that the upper limit of the characteristic pulsar ages is in the range from $\sim 10^9 - 3 \times 10^{10}$ yr. In principle, a better estimate of their age can be obtained from the determination of the cooling timescales of the white dwarf companion of those MSPs in binary systems. Amongst the MSPs in the Type I group with detectable X-ray emission, the cooling age of the white dwarf companion in J1012+5307 has been estimated to be less than 8×10^8 yrs (Hansen & Phinney 1998), significantly less than its pulsar characteristic age of $> 5.4 \times 10^9$ yr (Lorimer et al. 1995). However, uncertainties exist in such cooling ages since they sensitively depend on the thickness of the hydrogen-rich envelope especially for the cooling of low mass helium white dwarfs. For such white dwarfs hydrogen burning in the nondegenerate envelope can significantly prolong its lifetime (see, for example, Schönberner, Driebe, & Blöcker 2000) provided that thermally unstable shell flashes do not remove the outer layers (via Roche lobe overflow) to reduce the effectiveness of nuclear burning (Ergma, Sarna, & Gerskevits-Antipova 2001).

Given that the available observational evidence does not discriminate between the pulsar ages of the MSPs in Type I from those in Type II on a case by case basis, the differences in the duration of the post accretion phase are not well constrained. On the other hand, it is likely that the ages of the neutron stars in 47 Tuc are comparable to the age of the cluster corresponding to 11 - 13 Gyr (Schiavon et al. 2002) and are older than the neutron stars in the Type I group.

5. ORIGIN AND EVOLUTION OF MAGNETIC FIELDS

The hypothesis of strong small scale multipole fields at the neutron star surface provides a consistent interpretative framework for understanding the X-ray emission properties of the MSP of Type II. The existence of such fields in MSP is not new, however, since they had been suggested as possibly responsible for the complex profiles of MSPs (Krolik 1991). Furthermore, such fields have been hypothesized for facilitating copious production of e^\pm pairs required for pulsar emission in the seminal papers of Ruderman & Sutherland (1975) and Arons & Scharlemann (1979). Thus, their presence appears to be a common component in the phenomenology of pulsars. The creation of such fields may arise from thermal effects occurring in the thin layers of the crust (e.g., Blandford, Applegate, & Hernquist 1983; Arons 1993), from the coupling between various field components via the Hall effect during their

evolution (Shalybkov & Urpin 1997), or from rearrangement of the field, anchored in the core, due to crustal movements (Ruderman 1991a, 1991b).

Although an understanding of the origin and evolution of neutron star magnetic fields remains far from complete, observational evidence suggests that little field decay takes place during the active lifetime of a pulsar (i.e., before the pulsar reaches the death line) on timescales less than about a few times 10^8 yrs (Bhattacharya et al. 1992). Significant evolution of the magnetic field can take place, on the other hand, during a longer pre accretion phase or during the spin up phase associated with the accretion of matter (Konar & Bhattacharya 1997). Since the electrical conductivity in the neutron star core is very high, the evolutionary timescale for the magnetic field threading the core exceeds the Hubble timescale (Baym, Pethick, & Pines 1969). The magnetic field decay, therefore, reflects processes taking place in the crust. In this paper, we adopt the hypothesis that the magnetic field decay results from ohmic dissipation, rather than screening (Bisnovatyi-Kogan & Komberg 1974; Taam & van den Heuvel 1986; Romani 1990) which is susceptible to magnetic instabilities (Bhattacharya 2002; see also, Litwin, Brown & Rosner 2001). For a review on the current status of spontaneous and accretion induced magnetic evolution in neutron stars see the recent article by Bhattacharya (2002).

Since the pre accretion phase of neutron stars in globular clusters is likely to be significantly longer than the neutron stars in binaries in the Galactic field, it is likely that a crustal field can decay on timescales $\sim 10^9$ yr due to the finite electrical conductivity associated with the electron phonon scattering process in the deep crustal layers (Konar & Bhattacharya 1997). In this phase, the magnetic field can diffuse through the crust, perhaps embedding the complex field topology of the crustal layers into the denser regions, providing for a range of initial conditions for the field evolution that takes place in the following accretion phase.

When the neutron star accretes matter from its binary companion (via Roche lobe overflow) the magnetic field decay process can accelerate. This occurs after an isolated neutron star has acquired a companion as a result of an exchange collision with a primordial binary or via tidal capture in a globular cluster or as a result of the evolution of the binary itself in the Galactic field. The increase in the interior temperatures of the neutron star resulting from the compressional heating and nuclear burning lead to reduced electrical conductivities associated with the electron phonon scattering process. In contrast to the pre accretion phase, the ion electron scattering process can play a role and be more important than the electron phonon scattering process since the impurity content in the denser layers from nuclear burning can be increased (Schatz et al 1999), although the nuclear processing to Fe group nuclei that takes place during a superburst (Schatz, Bildsten, & Cumming 2003) may limit its importance. As a result a more rapid decay of the magnetic field takes place.

The decay process, however, is limited by the depth to which matter is accreted since the electrical conductivity increases in the denser layers which itself tends to decelerate the field decay process. The overall trend found by Konar & Bhattacharya (1997) reveals that, for a given initial dipole magnetic field, the fields decay to lower values for lower mass accretion rates. We note that the evolution of higher order magnetic fields has not been calculated for the accretion phase (which may, in part, be generated at the expense of low order fields by magnetic instabilities), although the evolution of a pre existing multipole field has been found to be similar to the dipole field, but on a shorter timescale, for the non accreting phase (Mitra, Konar, & Bhattacharya 1999).

After the accretion phase has ceased, the recycled neutron star re-enters the pulsar phase as a MSP with its magnetic field primarily residing in its core. Any further field evolution depends on flux expulsion from the core to the inner crustal regions as the neutron star slows down (Srinivasan et al. 1990; Bhattacharya & Srinivasan 1995). This field may reflect its pre existing topology, the diffusion of the field into the core during the pre accretion phase or the displacement of the crustal field into the core accompanying the replacement of the crust during accretion. However, the pulsar characteristic lifetime of several of the X-ray emitting MSPs discussed above can be long and the pulsar may not have spun down significantly suggesting that further field decay may be minimal. Hence, a picture emerges whereby the field decay depends on the evolutionary history of the MSP through its age, the amount of matter accreted by the neutron star, and the timescale on which the accretion takes place (e.g., Bhattacharya 2002).

Based on these rudimentary models for the magnetic field evolution, we hypothesize that the relative importance of the multipole fields is related to the long duration of the pre accretion phase in globular clusters. This hypothesis may be necessary, but is not sufficient to explain the disparity between the MSPs in Type I and Type II because of the existence of the MSPs in the globular clusters M28 and NGC 6397. If we assume that the neutron star in the MSP in M28 is formed in the same way as those in 47 Tuc and did not form recently as a result of an accretion induced collapse, perhaps leading to different initial field configurations, its existence would suggest that the emergence of the multipole field from the core at a stage when the neutron star is a MSP is delayed from the time that the accretion phase ceased. In other words, sufficient time must elapse for the multipole component of the core field to rediffuse through the crust to the surface. Since the core cools significantly after the accretion phase and the degree of impurities in the deep crust may be small, the timescale for rediffusion may exceed several Gyr.

As described in the previous section, the existence of the MSP in NGC 6397 does not lend itself to a straightforward interpretation unless it belongs to the Type I group similar

to the MSP in M28, except with a longer pulsar characteristic age. On the other hand, if it falls under the Type II category, then the multipole field must reemerge on timescales of $\lesssim 3 - 6 \times 10^8$ yrs. Recognizing that the pulsar ages are only upper limits, it is possible that some neutron stars in the Type I group have a longer MSP phase than the MSP in NGC 6397. This would present difficulties within the above framework and could imply that some MSP are so old that their multipole field has decayed during the post accretion phase. However, this may be considered unlikely since the field decay is ultimately determined by flux expulsion from the core during this phase. Because the spin down timescale is so long for the very old pulsars, little field decay is expected giving preference to the categorization for the MSP in NGC 6397 as Type I.

6. CONCLUSIONS

It has been shown that the X-ray properties of MSPs in 47 Tuc are distinct from other MSPs and normal radio pulsars. In particular, the X-ray spectra can be described by a black body model. For the inferred temperature and luminosity the emitting region is found to be significantly smaller than the polar cap X-ray area deduced from a dipolar magnetic field. In addition, the ratio of X-ray luminosity to spin down luminosity is abnormally low (about an order of magnitude lower), and the X-ray luminosity appears to exhibit a shallower dependence on spin period power. We suggest that the black body X-ray emission ($kT \sim 0.3$ keV), from very old MSPs (age $> 10^9$ yr) results from polar cap heating associated with the return current from the polar gap. Such temperatures result from models where the potential difference of the polar gap is insensitive to the observed pulsar global parameters, i.e., the rotation period and the dipolar magnetic field. A prediction of such models is that the thermal X-ray luminosity of the pulsar is roughly proportional to the square root of its own spin-down power. These models share one similarity, namely, the existence of a very strong surface magnetic field ($> 10^{12}$ G) of very small scale ($< 10^5$ cm). Such field strengths can follow from flux conservation arguments provided that the dipolar field lines and the surface field lines are connected, and the frame dragging effect (Asseo & Khechinashvili 2003) is important. Specifically, for a polar cap area $\sim s^2$, the surface field is $\sim 3 \times 10^{10} G \left(\frac{s}{3 \times 10^4 \text{ cm}}\right)^{-2} \left(\frac{B_d}{3 \times 10^8 G}\right) \left(\frac{P}{3 \times 10^{-3} \text{ s}}\right)^{-1}$. Furthermore, the general relativistic effect can amplify the surface magnetic field by a factor > 30 for multipole components of sufficiently high order (~ 5) (see Asseo & Khechinashvili 2003). If this interpretation is correct it imposes a very strong hint/constraint on the evolution of MSPs.

The hypothesis of multipole fields has also been invoked as a possible explanation for the existence of PSR J2144-3933 beyond the pulsar death line (see Young, Manchester, &

Johnston 1999; Gil & Mitra 2001). In addition, Becker et al. (2003) have recently found marginal evidence of an emission line centered at 3.3 keV from MSP PSR B1821-24. If this is identified as an electron cyclotron line, it implies a magnetic field, at least one hundred times stronger than its dipolar field.

We have suggested that most of the field MSPs with very old spin-down ages are probably young MSPs (e.g., PSR B1957+20, PSR J0751+1807). Therefore, the strong multipole field may not have had sufficient time to diffuse to the stellar surface in these pulsars. On the other hand, some field MSPs could be very old (e.g., PSR J1012+5307, PSR J1024-0719, PSR J1744-1134), but they may still lack a strong surface magnetic field. We speculate that this may relate to their actual age and/or the amount mass accreted from their companions. If the mass accreted is small, the multipole field may not anchor deeply inside the crust so it decays on a short time scale. On the other hand, the true age of these MSPs may not be as old as those MSPs in 47 Tuc. Confirmation of their actual age will provide further insight into the dependence of field evolution on their different formation histories (as hence initial magnetic field initial conditions) and their different pre-accretion, accretion, and post accretion phases.

We thank Drs. W. Becker, F. Camilo, J. Gil, W. Lewin, R.N. Manchester, E.S. Phinney, and N. Shibasaki for helpful comments. We are also grateful for the useful comments of the anonymous referee. This research was supported in part by a RGC grant of the Hong Kong Government to KSC and by NASA under grant NAG5-7011 and by the National Science Foundation under Grant No. AST-0200876 to RT.

REFERENCES

- Abrahams, A. M., & Shapiro, S. L. 1991, *ApJ*, 382, 233
- Alpar, M. A., Cheng, A. F., Ruderman, M. A., & Shaham, J. 1982, *Nature*, 300, 728
- Alpar, M. A., Pines, D., Anderson, P. W., & Shaham, J. 1984, *ApJ*, 276, 325
- Arons, J. 1981, *ApJ*, 248, 1099
- Arons, J. 1993, *ApJ*, 408, 160
- Arons, J., & Scharlemann, E. T. 1979, *ApJ*, 231, 854
- Asseo E., & Khechinashvili, D. 2003, *MNRAS*, 334, 743

- Bailyn, C. D., & Grindlay, J. E. 1987, *ApJ*, 316, L25
- Baym, G., Pethick, C., & Pines, D. 1969, *Nature*, 224, 675
- Becker, W. et al. 2003, *ApJ*, in press
- Becker, W. & Trümper, J. 1997, *A&A*, 326, 682
- Becker, W. & Trümper, J. 1999, *A&A*, 341, 803
- Bhattacharya, D. 2002, *JAA*, 22, 67
- Bhattacharya, D., & Srinivasan, G. 1995, *X-ray Binaries*, ed. W. H. G. Lewin, J. A. van Paradijs, & E. P. J. van den Heuvel (Cambridge: Cambridge University Press), 495
- Bhattacharya, D., Wijers, R. A. M. J., Hartman, J. W., & Verbunt, F. 1992, *A&A*, 254, 198
- Bisnovatyi-Kogan, G. S., & Komberg, B. V. 1974, *Sov. Astr.*, 18, 217
- Blandford, R. D., Applegate, J. H., & Hernquist, L. 1983, *MNRAS*, 204, 1025
- Camilo, F., Lorimer, D. R., Freire, P., Lyne, A. G., Manchester, R. N. 2000, *ApJ*, 535, 975
- Cheng, A. F., & Ruderman, M. A. 1980, *ApJ*, 235, 576
- Cheng, K. S., Chau, W. Y., Zhang, J. L., & Chau, H. F. 1992, *ApJ*, 396, 135
- Cheng, K. S., & Dai, Z. G. 1997, *ApJ*, 476, L39
- Cheng, K. S., Gil, J. & Zhang, L. 1997, *ApJ*, 493, L35
- Cheng, K. S., & Zhang, L. 1999, *ApJ*, 515, 337
- Cheng, K. S., Ho, C., & Ruderman, M. A. 1986, *ApJ*, 300, 500
- D’Amico, N., Possenti, A., Manchester, R. N., Sarkissian, J., Lyne, A. G., & Camilo, F. 2001, *ApJ*, 561, L89
- Daugherty, J. K., & Harding, A. K. 1996, *ApJ*, 458, 278
- Ergma, E., Sarna, M. J., & Gerskevits-Antipova, J. 2001, *MNRAS*, 321, 71
- Fan, G. L., Cheng, K. S., & Manchester, R. N. 2001, *ApJ*, 557, 297
- Freire, P. C., Camilo, F., Lorimer, D. R., Lyne, A. G., Manchester, R. N., & D’Amico, N. 2001, *MNRAS*, 326, 901

- Freire, P. C., Camilo, F., Kramer, M., Lorimer, D. R., Lyne, A. G., Manchester, R. N., & D'Amico, N. 2003, MNRAS, 340, 1359
- Galloway, D. K., Chakrabarty, D., Morgan, E. H., & Remillard, R. A. 2002, ApJ, 576, L137
- Gil, J., & Melikidze, G. K. 2002, ApJ, 577, 909
- Gil, J., & Mitra, D. 2001, ApJ, 550, 383
- Gil, J., & Sendyk, M. 2000, ApJ, 541, 351
- Goldreich, P. & Julian, W. H. 1969, ApJ, 157
- Grindlay, J. E., Camilo, F., Heinke, C. O., Edmonds, P. D., Cohn, H., & Lugger, P. 2002, ApJ, 581, 470
- Halpern, J. P., & Ruderman, M. 1993, ApJ, 415, 286
- Hansen, B. M. S., Kalogera, V. & Rasio, F. A. 2003, ApJ, 415, 286
- Hansen, B. M. S., & Phinney, E. S. 1998, MNRAS, 294, 569
- Harding, A. K., Muslimov, A. G., & Zhang, B. 2002, ApJ, 576, 376
- Harding, A. K., Ozernoy, L. M., Usov, V. V. 1993, MNRAS, 265, 921
- Heggie, D. C. 1975, MNRAS, 173, 729
- Hut, P. 1984, ApJS, 55, 11
- Jones, P. B. 1980, MNRAS, 192, 847
- Jones, P. B. 1986, MNRAS, 222, 577
- Konar, S., & Bhattacharya, D. 1997, MNRAS, 284, 311
- Krolik, J. 1991, ApJ, 373, L69
- Li, X. D. 2002, ApJ, 564, 930
- Litwin, C., Brown, E.F., & Rosner, R. 2001, ApJ, 553, 788
- Lorimer, D. R., Lyne, A. G., Festin, L., & Nicastro, L. 1995, Nature, 376, 393
- Lyne, A. G., Brinklow, A., Middleditch, J., Kulkarni, S. R., Backer, D. C., & Clifton, T. R. 1987, Nature, 328, 399

- Markwardt, C. B., Smith, E., & Swank, J. H. 2003, IAU Circ. No. 8080
- Markwardt, C., Swank, J. H., Strohmayer, T. E., Zand, J. J. M. in't, & Marshall, F. E. 2002, ApJ, 575, L21
- Michel, F. C. 1991, ApJ, 383, 808
- Mineo, T. et al. 2000, A&A, 355, 1053
- Mitra, D., Konar, S., & Bhattacharya, D. 1999, MNRAS, 307, 459
- Phinney, E. S. & Kulkarni, S. R. 1994, ARA&A, 32, 591
- Podsiadlowski, Ph., Rappaport, S., & Pfahl, E. D. 2002, ApJ, 565, 1107
- Radhakrishnan, V. & Srinivasan, G. 1982, Curr. Sci., 51, 1096
- Rasio, F., Pfahl, E. D., & Rappaport, S. 2000, ApJ, 532, L47
- Romani, R. 1990, Nature, 347, 741
- Ruderman, M. 1991a, ApJ, 366, 261
- Ruderman, M. 1991b, ApJ, 382, 576
- Ruderman, M. & Cheng, K. S. 1988, ApJ, 335, 306
- Ruderman, M. A., & Sutherland, P. G. 1975, ApJ, 196, 51
- Saito, Y. et al. 1997, ApJ, 477, L37
- Sakurai, I. et al. 2001, PASJ, 53, 535
- Scharlemann, E. T., Arons, J., & Fawley, W. M. 1978, ApJ, 222, 297
- Schatz, H., Bildsten, L, & Cumming, A. 2003, ApJ, 583, L87
- Schatz, H., Bildsten, L, Cumming, A., & Wiescher, M. 1999, ApJ, 524, 1014
- Schiavon, R. P., Faber, S. M., Rose, J. A., & Castilho, B. V. 2002, ApJ, 580, 873
- Schönberner, D., Driebe, T., & Blöcker, T. 2000, A&A, 356, 929
- Shalybkov, D. A., & Urpin, V. A. 1997, A&A, 321, 685
- Shibazaki, N., & Lamb, F. K. 1988, ApJ, 346, 808

- Srinivasan, G. et al. 1990, *Curr. Sci.*, 59, 31
- Stappers, B.W., Gaensler, B.M., Kaspi, V.M., van der Klis, M., & Lewin, W. H. G. 2003, *Science*, 299, 1372
- Taam, R. E., King, A. R., & Ritter, H. 2000, *ApJ*, 541, 329
- Taam, R. E., & Lin, D. N. C. 1992, *ApJ*, 390, 440
- Taam, R. E., & Sandquist, E. L. 2000, *ARA&A*, 38, 113
- Taam, R. E., & van den Heuvel, E. P. J. 1986, *ApJ*, 305, 235
- Takahashi, M. et al. 2001, *ApJ*, 554, 316
- Tennant, A.F. et. al. 2001, *ApJ*, 554, 173
- Tsuruta, S. 1998, *Phy. Rep.*, 292, 1
- Usov, V. V., & Melrose, D. B. 1995, *AuJPh.*, 48, 571
- van den Heuvel, E. P., van Paradijs, J. A., & Taam, R. E. 1986, *Nature*, 322, 153
- Wijnands, R., & van der Klis, M. 1998, *Nature*, 394, 344
- Young, M. D., Manchester, R. N., & Johnston, S. 1999, *Nature*, 400, 848
- Woosley, S.E., Heger, A., & Weaver, T.A. 2002, *Rev. Mod. Phys.*, 74, 1015
- Zavlin, v. E., Pavlov, G. G., Sanwal, D., Manchester, R. N., & Trümper, J. 2002, *ApJ*, 569, 894

Table 1. Comparison between the observed X-ray luminosity and model predictions.

	L_X^{obs} (10^{29}) erg s $^{-1}$		L_X^{RS} (10^{31}) erg s $^{-1}$		L_X^{CZ} (10^{29}) erg s $^{-1}$		L_X^{Jones} (10^{29}) erg s $^{-1}$		L_X^A (10^{29}) erg s $^{-1}$	
	(a)	(b)	(a)	(b)	(a)	(b)	(a)	(b)	(a)	(b)
47Tuc-C	3.98	1.28 ($\frac{1.72}{1.16}$)	2.19	5.19 ($\frac{7.33}{4.62}$)	9.69	2.79 ($\frac{3.95}{2.49}$)	5.22	5.32 ($\frac{7.52}{4.74}$)	9.95	
47Tuc-D	19.95	2.16 ($\frac{2.90}{1.96}$)	4.62	9.22 ($\frac{13.03}{8.22}$)	22.39	4.97 ($\frac{7.02}{4.43}$)	12.06	10.54 ($\frac{14.89}{9.40}$)	25.59	
47Tuc-E	39.81	5.68 ($\frac{7.64}{5.15}$)	11.25	23.17 ($\frac{32.73}{20.65}$)	51.38	12.48 ($\frac{17.63}{11.12}$)	27.67	49.38 ($\frac{69.76}{44.01}$)	109.51	
47Tuc-F	31.62	5.85 ($\frac{7.87}{5.30}$)	19.02	20.65 ($\frac{29.17}{18.40}$)	81.68	11.12 ($\frac{15.71}{9.91}$)	43.99	68.88 ($\frac{97.29}{61.39}$)	272.44	
47Tuc-G	12.59	2.44 ($\frac{3.28}{2.21}$)	7.54	9.22 ($\frac{13.03}{8.22}$)	34.44	4.97 ($\frac{7.02}{4.43}$)	18.55	16.10 ($\frac{22.74}{14.35}$)	60.11	
47Tuc-H	12.59	1.64 ($\frac{2.21}{1.49}$)	9.25	5.19 ($\frac{7.33}{4.62}$)	38.96	2.79 ($\frac{3.95}{2.49}$)	20.99	12.78 ($\frac{18.05}{11.39}$)	96.02	
47Tuc-I	15.85	3.16 ($\frac{4.25}{2.87}$)	9.07	11.61 ($\frac{16.40}{10.35}$)	39.68	6.25 ($\frac{8.83}{5.57}$)	21.37	25.30 ($\frac{35.74}{22.55}$)	86.45	
47Tuc-J	19.95	6.44 ($\frac{8.66}{5.83}$)	10.47	20.65 ($\frac{29.17}{18.40}$)	36.40	11.12 ($\frac{15.71}{9.91}$)	19.61	96.14 ($\frac{135.80}{85.68}$)	169.48	
47Tuc-L	25.12	3.87 ($\frac{5.20}{3.51}$)	6.45	16.40 ($\frac{23.17}{14.62}$)	29.76	8.83 ($\frac{12.48}{7.87}$)	16.03	25.66 ($\frac{36.25}{22.87}$)	46.56	
47Tuc-M	12.59	2.08 ($\frac{2.80}{1.89}$)	4.46	7.33 ($\frac{10.35}{6.53}$)	17.82	3.95 ($\frac{5.57}{3.52}$)	9.60	14.73 ($\frac{20.81}{13.13}$)	35.84	
47Tuc-N	15.85	4.08 ($\frac{5.48}{3.70}$)	10.30	14.62 ($\frac{20.65}{13.03}$)	43.06	7.87 ($\frac{11.12}{7.02}$)	23.19	38.83 ($\frac{54.84}{34.60}$)	114.35	
47Tuc-O	39.81	5.83 ($\frac{7.84}{5.29}$)	18.72	20.65 ($\frac{29.17}{18.40}$)	80.46	11.12 ($\frac{15.71}{9.91}$)	43.34	68.11 ($\frac{96.20}{60.70}$)	265.38	
47Tuc-Q	12.59	4.41 ($\frac{5.93}{4.00}$)	7.57	18.40 ($\frac{26.00}{16.40}$)	34.56	9.91 ($\frac{14.00}{8.83}$)	18.62	32.21 ($\frac{45.49}{28.70}$)	60.48	
47Tuc-T	10.00	2.05 ($\frac{2.76}{1.86}$)	5.21	10.35 ($\frac{14.62}{9.22}$)	30.68	5.57 ($\frac{7.87}{4.97}$)	16.53	7.02 ($\frac{9.91}{6.25}$)	20.81	
47Tuc-U	19.95	3.87 ($\frac{5.20}{3.51}$)	8.01	16.40 ($\frac{23.17}{14.62}$)	38.33	8.83 ($\frac{12.48}{7.87}$)	20.64	25.69 ($\frac{36.29}{22.90}$)	60.03	

Note: (a) Grindlay et. al. 2002 (b) Freire et. al. 2001

Table 1—Continued

	L_X^{obs} (10^{29}) erg s $^{-1}$	L_X^{CR} (10^{18}) erg s $^{-1}$	$L_X^{HM(R)}$ (10^{34}) erg s $^{-1}$	$L_X^{HM(NR)}$ (10^{31}) erg s $^{-1}$			
		(a)	(b)	(a)	(b)	(a)	(b)
47Tuc-C	3.98	1.87 ($\frac{5.14}{1.34}$)	11.64	26.74 ($\frac{18.93}{30.01}$)	14.31	1.44 ($\frac{1.44}{1.44}$)	1.44
47Tuc-D	19.95	7.11 ($\frac{19.49}{5.08}$)	94.68	19.34 ($\frac{13.69}{21.70}$)	7.97	1.61 ($\frac{1.61}{1.61}$)	1.61
47Tuc-E	39.81	14.02 ($\frac{38.43}{10.02}$)	143.44	32.95 ($\frac{23.33}{36.97}$)	14.86	3.00 ($\frac{3.00}{3.00}$)	3.00
47Tuc-F	31.62	2.36 ($\frac{6.47}{1.69}$)	130.91	105.12 ($\frac{74.42}{117.95}$)	26.58	4.69 ($\frac{4.69}{4.69}$)	4.69
47Tuc-G	12.59	1.81 ($\frac{4.97}{1.30}$)	85.01	51.92 ($\frac{36.76}{58.26}$)	13.91	2.45 ($\frac{2.45}{2.45}$)	2.45
47Tuc-H	12.59	0.11 ($\frac{0.30}{0.08}$)	40.05	206.49 ($\frac{146.19}{231.69}$)	27.49	3.46 ($\frac{3.46}{3.46}$)	3.46
47Tuc-I	15.85	1.74 ($\frac{4.76}{1.24}$)	62.83	69.20 ($\frac{48.99}{77.65}$)	20.25	3.06 ($\frac{3.06}{3.06}$)	3.06
47Tuc-J	19.95	0.81 ($\frac{2.21}{0.58}$)	4.22	228.88 ($\frac{162.03}{256.81}$)	129.83	6.54 ($\frac{6.54}{6.54}$)	6.54
47Tuc-L	25.12	13.87 ($\frac{38.03}{9.91}$)	79.03	22.62 ($\frac{16.01}{25.38}$)	12.46	2.20 ($\frac{2.20}{2.20}$)	2.20
47Tuc-M	12.59	0.59 ($\frac{1.61}{0.42}$)	7.87	90.94 ($\frac{64.38}{102.04}$)	37.38	2.83 ($\frac{2.83}{2.83}$)	2.83
47Tuc-N	15.85	1.80 ($\frac{4.93}{1.28}$)	42.10	87.26 ($\frac{61.78}{97.91}$)	29.63	3.73 ($\frac{3.73}{3.73}$)	3.73
47Tuc-O	39.81	2.45 ($\frac{6.71}{1.75}$)	129.93	102.40 ($\frac{72.49}{114.89}$)	26.28	4.64 ($\frac{4.64}{4.64}$)	4.64
47Tuc-Q	12.59	13.52 ($\frac{37.07}{9.66}$)	85.16	26.19 ($\frac{18.54}{29.38}$)	13.94	2.46 ($\frac{2.46}{2.46}$)	2.46
47Tuc-T	10.00	53.66 ($\frac{147.11}{38.34}$)	1282.06	5.10 ($\frac{3.61}{5.72}$)	1.72	0.95 ($\frac{0.95}{0.95}$)	0.95
47Tuc-U	19.95	13.82 ($\frac{37.89}{9.87}$)	164.74	22.68 ($\frac{16.06}{25.45}$)	9.71	2.20 ($\frac{2.20}{2.20}$)	2.20

Note: (a) Grindlay et. al. 2002 (b) Freire et. al. 2001

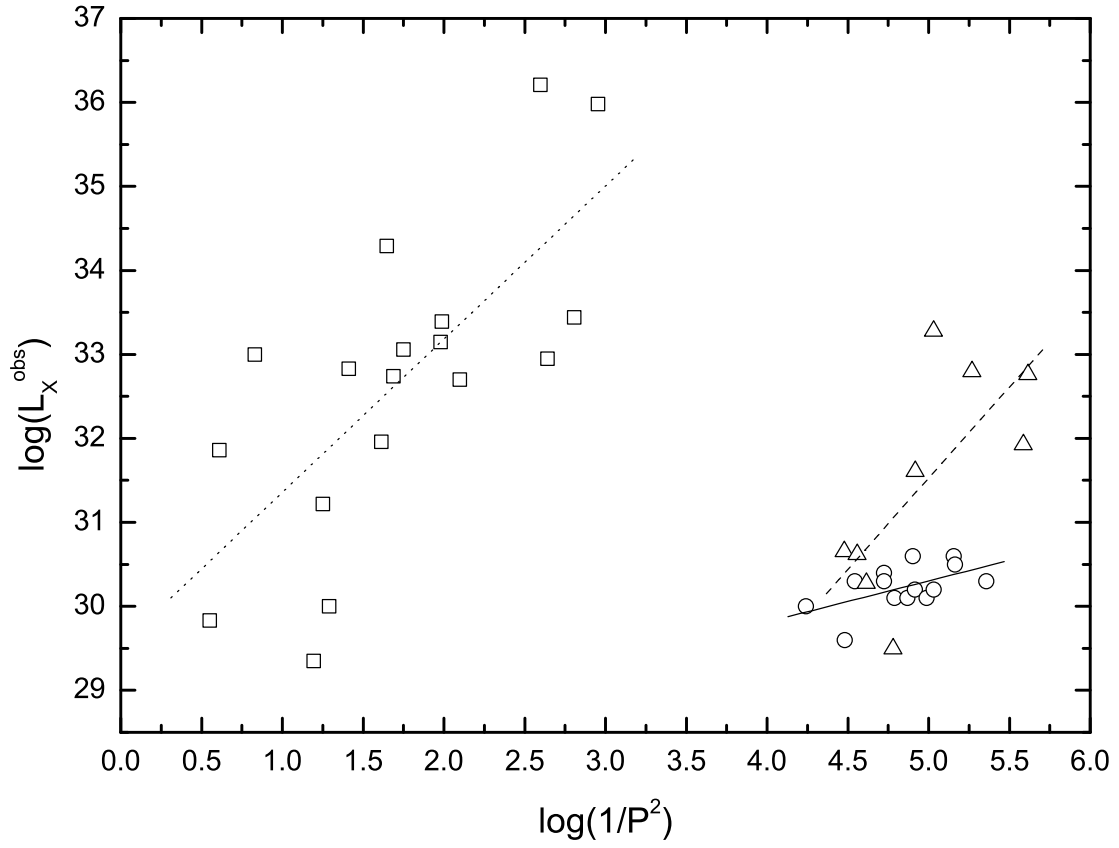


Fig. 1.— The plot of the observed X-ray luminosity versus $1/P^2$. The squares represent normal radio pulsars (Becker & Trümper 1997), the triangles represent MSPs excluding those in 47 Tuc (Becker & Trümper 1999), and the circles represent MSPs in 47 Tuc (Grindlay et. al. 2002).

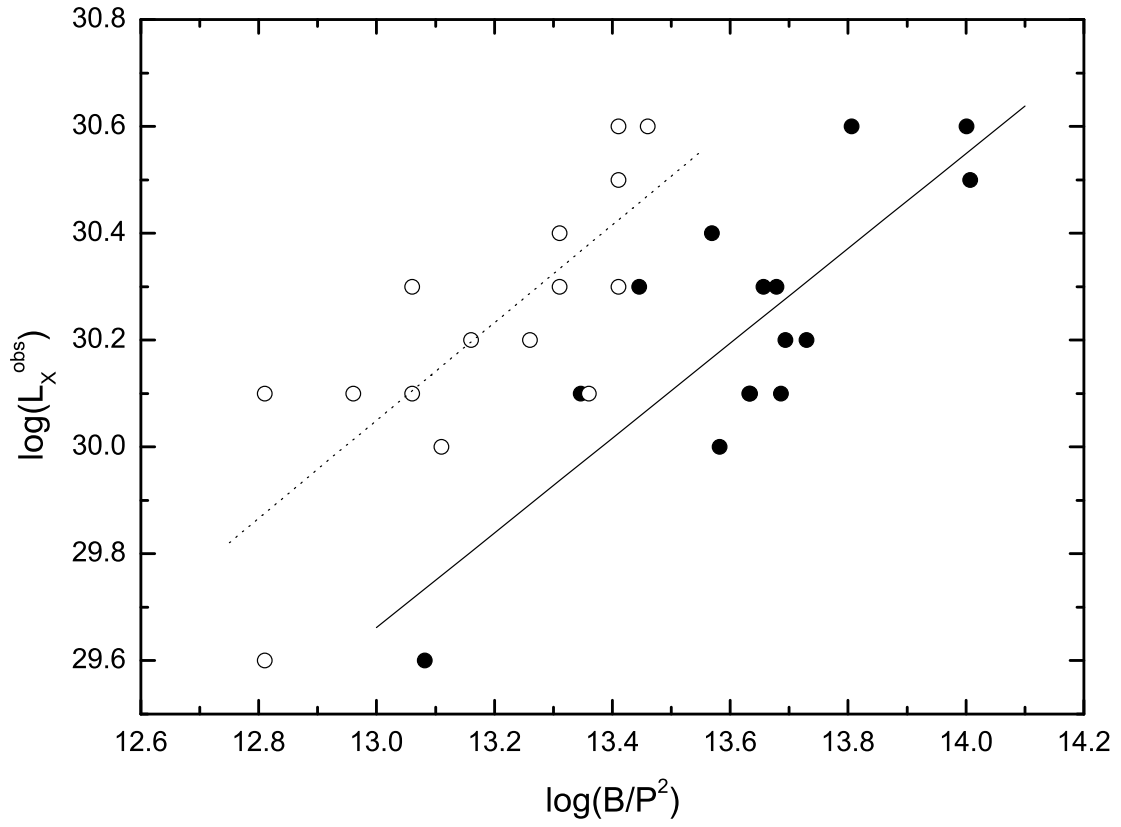


Fig. 2.— The plot of observed X-ray luminosity versus B/P^2 . The circles represent data using magnetic fields estimated by Grindlay et. al. (2002) and dots represent data using magnetic fields estimated by Freire et. al. (2001).